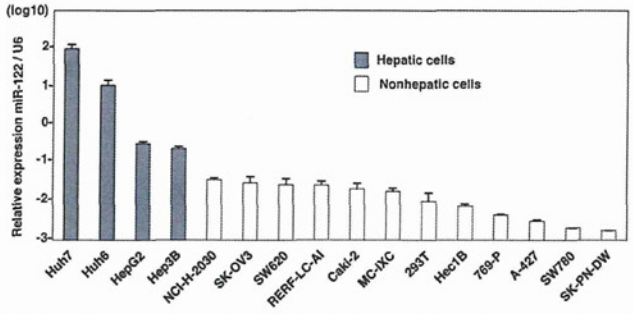

FIG 1 Endogenous expression levels of miR-122 in hepatic and nonhepatic cells. Total miRNAs were extracted from Huh7, Huh6, HepG2, Hep3B, NCI-H-2030, SK-OV3, SW620, RERF-LC-AI, Caki-2, MC-IXC, 293T, Hec1B, 769-P, A-427, SW780, and SK-PN-DW cells, and the expression levels of miR-122 were determined by qRT-PCR.

nonpermissive for HCVcc propagation (29, 43). These results suggest that the high susceptibility of Huh7 cells to the propagation of HCVcc is attributable to the high expression level of miR-122 and raise the possibility of expanding the HCV host range through the exogenous expression of miR-122 in nonhepatic cells.

In this study, we assessed the effect of miR-122 expression on the replication of HCVcc and SGR RNA in several nonhepatic cell lines. Although the exogenous expression of miR-122 in the cell lines facilitates significant RNA replication through a gene-specific interaction between miR-122 and 5′ UTR of HCV RNA, no infectivity was detected in either the cells or the culture supernatants. The current study suggests that the expression of miR-122 plays an important role in HCV cell tropism, as well as in the possible involvement of nonhepatic cells in EHM, through an incomplete propagation of HCV.

MATERIALS AND METHODS

NextBio Body Atlas. The NextBio Body Atlas application presents an aggregated analysis of gene expression across various normal tissues, normal cell types, and cancer cell lines. It enables us to investigate the expression of individual genes as well as gene sets. Samples for Body Atlas data are obtained from publicly available studies that are internally curated, annotated, and processed (31). Body Atlas measurements are generated from all available RNA expression studies that used Affymetrix U133 Plus or U133A Genechip arrays for human studies. The results corresponding to 128 human tissue samples were incorporated from 1,067 arrays, the results corresponding to 157 human cell types were incorporated from 1,474 arrays, and the results corresponding to 359 human cancer cell lines were incorporated from 376 arrays. Gene queries return a list of relevant tissues or cell types rank ordered by absolute gene expression and grouped by body systems or across all body systems. In the current analysis, we screened for nonhepatic cell lines expressing HCV receptor candidates, including CD81, SR-BI, claudin1 (CLDN1), and occludin (OCLN), or very-low-density lipoprotein (VLDL)-associated proteins, including apolipoprotein E (ApoE), ApoB, and microsomal triglyceride transfer protein (MTTP). A detailed analysis protocol developed by NextBio was described previously (31). The raw data used in this application are derived from the GSK Cancer Cell Line data deposited at the National Cancer Institute website (https://array.nci.nih.gov/caarray/project/woost-00041) and additionally from NCBI Gene Expression Omnibus (GEO) accession number GSE5720 for cell lines SK-OV-3 and SW620.

Sample collection and RNA extraction for microarray analysis. Total RNAs extracted from cells were purified by using an miRNeasy kit (Qiagen, Valencia, CA) according to the manufacturer's protocol. Eluted RNAs were quantified using a Nanodrop ND-1000 (version 3.5.2) spectrophotometer (Thermo Scientific, Wartham, MA). RNA integrity was evaluated using the RNA 6000 LabChip kit and bioanalyzer (Agilent Technologies, Santa Clara, CA). Each RNA that had an RNA integrity number (RIN) greater than 9.0 was used for the microarray experiments.

Microarray experiment. Expression profiling was generated using the 4 × 44K whole-human-genome oligonucleotide microarray (version 2.0) G4845A (Agilent Technologies). Each microarray uses 44,495 probes to interrogate 27,958 Entrez gene RNAs. One hundred nanograms of total RNA was reverse transcribed into double-stranded cDNAs by AffinityScript multiple-temperature reverse transcriptase and amplified for 2 h at 40°C. The resulting cDNAs were subsequently used for *in vitro* transcription by the T7 polymerase and labeled with cyanine-3-labeled cytosine triphosphate (Perkin Elmer, Waltham, MA) for 2 h at 40°C using a low-input Quick-Amp labeling kit (Agilent Technologies) according to the manufacturer's protocol. After labeling, the rates of dye incorporation and quantification were measured with a Nanodrop ND-1000 (version 3.5.2) spectrophotometer (Thermo Scientific), and then the cRNAs were fragmented for 30 min at 60°C in the dark. Differentially labeled samples of 1,650 ng of cRNA were hybridized on Agilent 4 × 44K whole-genome arrays (version 2.0; 026652; Agilent Design) at 65°C for 17 h with rotation in the dark. Hybridization was performed using a gene expression hybridization kit (Agilent Technologies) following the manufacturer's instructions. After washing in gene expression washing buffer, each slide was scanned with the Agilent microarray scanner G2505C. Feature extraction software (version 10.5.1.1) employing defaults for all parameters was used to convert the images into gene expression data. Raw data were imported into a Subio platform (version 1.12) for database management and quality control. Raw intensity data were normalized against GAPDH (glyceraldehyde-3-phosphate dehydrogenase) expression levels for further analysis. These raw data have been accepted by GEO (a public repository for microarray data aimed at storing minimum information about microarray experiments [MIAME]).

Plasmids. The cDNA clones of wild-type (WT) and mutant (MT) pri-miR-122 and *Aequorea coerulescens* green fluorescent protein (AcGFP) were inserted between the XhoI and XbaI sites of lentiviral vector pCSII-EF-RfA, which was kindly provided by M. Hijikata, and the resulting plasmids were designated pCSII-EF-WT-miR-122, pCSII-EF-MT-miR-122, and pCSII-EF-AcGFP, respectively. Plasmids pHH-JFH1 and pSGR-JFH1, which encode full-length and subgenomic cDNA of the JFH1 strain, respectively, were kindly provided by T. Wakita. pHH-JFH1-E2p7NS2mt contains three adaptive mutations in pHH-JFH1 (53). pHH-JFH1-M1 and pHH-JFH1-M2 were established by the introduction of a point mutation of nucleotide 26 located in site 1 and nucleotide 41 in site 2 of the 5′ UTR of the JFH1 cDNA construct pHH-JFH1. pSGR-Con1, which encodes SGR of the Con1 strain, was kindly provided by R. Bartenschlager. The complementary sequences of miR-122 were introduced into the multicloning site of the pmirGLO vector (Promega, Madison, WI), and the resulting plasmid was designated pmirGLO-compl-miR-122. The plasmids used in this study were confirmed by sequencing with an ABI 3130 genetic analyzer (Applied Biosystems, Tokyo, Japan).

Cell lines. All cell lines were cultured at 37°C under the conditions of a humidified atmosphere and 5% CO_2. The following cells were maintained in Dulbecco modified Eagle medium (DMEM; Sigma-Aldrich, St. Louis, MO) supplemented with 100 U/ml penicillin, 100 μg/ml streptomycin, and 10% fetal calf serum (FCS): human hepatocellular carcinoma-derived Huh7, Hep3B, and HepG2; embryonic kidney-derived HEK293 and 293T; lung-derived RERF-LC-AI, NCI-H-2030, and A-427; kidney-derived Caki-2 and 769-P; neuron-derived MC-IXC and SK-PN-DW; uterus-derived Hec1B; ovary-derived SK-OV3; colon-derived SW620; and urinary bladder-derived SW780 cells. RERF-LC-AI (RCB0444) cells were provided by the RIKEN BRC through the National Bio-Resource Project of MEXT, Japan. Hec1B (JCRB1193) cells were obtained from the JCRB Cell Bank. NCI-H-2030, A-427, Caki-2, 769-P, MC-IXC, SK-PN-DW, SK-OV3, and SW780 cells were obtained from the American Type Culture Collection (ATCC). SW620 cells were kindly provided by C.

Oneyama. 293T-CLDN cells stably expressing CLDN1 were established by the introduction of the expression plasmids encoding CLDN1 under the control of the CAG promoter of pCAG-pm3. The Huh7-derived cell line Huh7.5.1 was kindly provided by F. Chisari. The Huh7OK1 cell line efficiently propagates HCVcc as previously described (45). Huh7, Hec1B, and HEK293 cells harboring Con1- or JFH1-based HCV SGR were prepared according to the method described in a previous report (47) and maintained in DMEM containing 10% FCS and 1 mg/ml G418 (Nakalai Tesque, Kyoto, Japan).

Antibodies and drugs. Mouse monoclonal antibodies to HCV nonstructural protein 5A (NS5A) and β-actin were purchased from Austral Biologicals (San Ramon, CA) and Sigma-Aldrich, respectively. Mouse anti-ApoE antibody was purchased from Santa Cruz Biotechnology (Santa Cruz, CA). Rabbit anti-HCV core protein and NS5A were prepared as described previously (41). Rabbit anti-SR-BI antibody was purchased from Novus Biologicals (Littleton, CO). Rabbit anti-CLDN1 and -OCLN antibodies, Alexa Fluor 488 (AF488)-conjugated anti-rabbit or -mouse IgG antibodies, and AF594-conjugated anti-mouse IgG2a antibodies were purchased from Invitrogen (San Diego, CA). Mouse anti-FKBP8 antibody was described previously (44). Mouse anti-double-stranded RNA (anti-dsRNA) IgG2a (J1 and K2) antibodies were obtained from Biocenter Ltd. (Szirak, Hungary). The HCV NS3/4A protease inhibitor was purchased from Acme Bioscience (Salt Lake City, UT). Human recombinant alpha IFN (IFN-α) and cyclosporine were purchased from PBL Biomedical Laboratories (Piscataway, NJ) and Sigma-Aldrich, respectively. BODIPY 558/568 lipid probe was purchased from Invitrogen. The locked nucleic acid (LNA) targeted to miR-122, LNA-miR-122 (5′-CcAttGTcaCaCtCC-3′), and its negative control, LNA-control (5′-CcAttCTgaCcCtAC-3′) (LNAs are in capital letters, DNAs are in lowercase letters; sulfur atoms in oligonucleotide phosphorothioates are substituted for nonbridging oxygen atoms; the capital C indicates LNA methylcytosine), were purchased from Gene Design (Osaka, Japan) (15).

Preparation of viruses. pHH-JFH1-E2p7NS2mt was introduced into Huh7.5.1 cells, HCVcc in the supernatant was collected after serial passages (39), and infectious titers were determined by a focus-forming assay and expressed in focus-forming units (FFUs) (62). Mutant HCVcc was produced from Huh7.5.1 cells expressing MT miR-122 according to the method of a previous report with minor modifications (25). HCVpv, a pseudotype vesicular stomatitis virus (VSV) bearing HCV E1 and E2 glycoproteins, was prepared as previously described (61), and infectivity was assessed by luciferase expression on a Bright-Glo luciferase assay system (Promega), following a protocol provided by the manufacturer and expressed in relative light units (RLUs).

Lipofection and lentiviral gene transduction. Cells were transfected with the plasmids by using Trans IT LT-1 transfection reagent (Mirus, Madison, WI) according to the manufacturer's protocol. LNAs were introduced into cells by Lipofectamine RNAiMAX (Invitrogen). The lentiviral vectors and ViraPower lentiviral packaging mix (Invitrogen) were cotransfected into 293T cells, and the supernatants were recovered at 48 h posttransfection. The lentivirus titer was determined by a Lenti-XTM quantitative reverse transcription-PCR (qRT-PCR) titration kit (Clontech, Mountain View, CA), and the expression levels of miR-122 and AcGFP were determined at 48 h postinoculation.

Quantitative RT-PCR. HCV RNA levels were determined by the method described previously (18). Total RNA was extracted from cells by using an RNeasy minikit (Qiagen). The first-strand cDNA synthesis and qRT-PCR were performed with TaqMan EZ RT-PCR core reagents and an ABI Prism 7000 system (Applied Biosystems), respectively, according to the manufacturer's protocols. The primers for TaqMan PCR targeted to the noncoding region of HCV RNA were synthesized as previously reported (42). To determine the expression levels of miR-122, total miRNA was prepared by using the miRNeasy minikit, and miR-122 expression was determined by using fully processed miR-122-specific RT and PCR primers provided in the TaqMan microRNA assays according to the manufacturer's protocol. U6 small nuclear RNA was used as an internal control. Fluorescent signals were analyzed with the ABI Prism 7000 system.

Immunoblotting. Cells were lysed on ice in lysis buffer (20 mM Tris-HCl [pH 7.4], 135 mM NaCl, 1% Triton X-100, 10% glycerol) supplemented with a protease inhibitor mix (Nacalai Tesque). The samples were boiled in loading buffer and subjected to 5 to 20% gradient SDS-PAGE. The proteins were transferred to polyvinylidene difluoride membranes (Millipore, Bedford, MA) and reacted with the appropriate antibodies. The immune complexes were visualized with SuperSignal West Femto substrate (Pierce, Rockford, IL) and detected with an LAS-3000 image analyzer system (Fujifilm, Tokyo, Japan).

Immunofluorescence assay. Cells cultured on glass slides were fixed with 4% paraformaldehyde (PFA) in phosphate-buffered saline (PBS) at room temperature for 30 min, permeabilized for 20 min at room temperature with PBS containing 0.2% Triton, after being washed three times with PBS, and blocked with PBS containing 2% FCS for 1 h at room temperature. The cells were incubated with PBS containing appropriate primary antibodies at room temperature for 1 h, washed three times with PBS, and incubated with PBS containing AF488- or AF594-conjugated secondary antibodies at room temperature for 1 h. For lipid droplet staining, cells incubated in medium containing 20 μg/ml BODIPY for 20 min at 37°C were washed with prewarmed fresh medium and incubated for 20 min at 37°C. Cell nuclei were stained with DAPI (4′,6-diamidino-2-phenylindole). Cells were observed with a FluoView FV1000 laser scanning confocal microscope (Olympus, Tokyo, Japan).

***In vitro* transcription, RNA transfection, and colony formation.** The plasmids pSGR-Con1 and pSGR-JFH1 were linearized with ScaI and XbaI, respectively, and treated with mung bean exonuclease. The linearized DNA was transcribed *in vitro* by using a MEGAscript T7 kit (Applied Biosystems) according to the manufacturer's protocol. The *in vitro*-transcribed RNA (10 μg) was electroporated into Hec1B and HEK293 cells at 10^7 cells/0.4 ml under conditions of 190 V and 975 μF using a Gene Pulser apparatus (Bio-Rad, Hercules, CA) and plated on DMEM containing 10% FCS. The medium was replaced with fresh DMEM containing 10% FCS and 1 mg/ml G418 at 24 h posttransfection. The remaining colonies were cloned by using a cloning ring (Asahi Glass, Tokyo, Japan) or fixed with 4% PFA and stained with crystal violet at 4 weeks postelectroporation.

Electron microscopy and correlative FM-EM analysis. Cells were cultured on a Cell Desk polystyrene coverslip (Sumitomo Bakelite) and were fixed with 2% formaldehyde and 2.5% glutaraldehyde in 0.1 M cacodylate buffer (pH 7.4) containing 7% sucrose. Cells were postfixed for 1 h with 1% osmium tetroxide and 0.5% potassium ferrocyanide in 0.1 M cacodylate buffer (pH 7.4), dehydrated in graded series of ethanol, and embedded in Epon812 (TAAB). Ultrathin (80-nm) sections were stained with saturated uranyl acetate and lead citrate solution. Electron micrographs were obtained with a JEM-1011 transmission electron microscope (JEOL). Correlative fluorescence microscopy (FM)-electron microscopy (EM) allows individual cells to be examined both in an overview with FM and in a detailed subcellular-structure view with EM (51). The NS5A was stained and observed in the Hec1B-derived Con1 SGR cells by the correlative FM-EM method as described previously (44).

Intracellular infectivity. Intracellular viral titers were determined according to a method previously reported (20). Briefly, cells were extensively washed with PBS, scraped, and centrifuged for 5 min at 1,000 × *g*. Cell pellets were resuspended in 500 μl of DMEM containing 10% FCS and subjected to three cycles of freezing and thawing using liquid nitrogen and a thermo block set to 37°C. Cell lysates were centrifuged at 10,000 × *g* for 10 min at 4°C to remove cell debris. Cell-associated infectivity was determined by a focus-forming assay.

Statistical analysis. The data for statistical analyses are averages of three independent experiments. Results were expressed as means ± standard deviations. The significance of differences in the means was determined by Student's *t* test.

Microarray data accession number. Access to data concerning this study may be found under GEO experiment accession number GSE32886.

RESULTS

Nonhepatic cell lines susceptible to HCVcc by expression of miR-122. Human CD81 (hCD81), SR-B1, CLDN1, and OCLN are crucial for HCV entry (16, 48, 49, 56). First, we examined the expression of these receptor candidates in nonhepatic cell lines by using the web-based NextBio search engine (Cupertino, CA). Multidimensional scaling was used to visualize the differences in expression patterns of molecules of various tissues, cells, and cell lines from those of hepatic cell lines and primary hepatocytes. We selected nine nonhepatic cell lines as possibly being susceptible to HCVcc infection: NCI-H-2030 (lung), Caki-2 (kidney), 769-P (bladder), A-427 (lung), SK-OV3 (ovary), SW780 (bladder), SW620 (colon), RERF-LC-AI (lung), and Hec1B (uterus) (Fig. 2). In addition, three nonhepatic cell lines previously reported to be susceptible to replication of HCV RNA—that is, SK-PN-DW (neuron), MC-IXC (neuron), and 293T-CLDN (kidney)—were included in this study (8, 17). The expression of each receptor molecule in these 12 nonhepatic cell lines was confirmed by fluorescence-activated cell sorter (FACS) analysis and immunoblotting (Fig. 3A and B). To examine the expression of the functional receptors for HCV entry in these cell lines, we inoculated HCVpv into the cells. Ten of the cell lines (A-427 and SW780 being the exceptions) exhibited various degrees of susceptibility to HCVpv infection (Fig. 3C). Therefore, we examined the possibility of propagation of HCVcc by the expression of miR-122 in these 10 cell lines.

To introduce miR-122 in the cell lines, we employed a lentiviral vector encoding pri-miR-122, an unprocessed miR-122. To confirm the maturation of pri-miR-122 to form functional RNA-induced silencing complexes (RISCs), suppression of the translation of the target mRNA was determined by a dual reporter assay. Translation of a firefly luciferase mRNA containing the sequences complementary to miR-122 in the 3′ UTR was suppressed by infection with the lentivirus encoding pri-miR-122 but not by infection with a control virus (data not shown), suggesting that the pri-miR-122 is processed into a functionally mature miR-122. By using this lentiviral vector, high levels of miR-122 expression were achieved in the 10 cell lines, comparable to the endogenous expression level of miR-122 in Huh7 cells (Fig. 4A).

To examine the effect of the exogenous expression of miR-122 on HCV replication, the nonhepatic cell lines expressing miR-122 were infected with HCVcc at a multiplicity of infection (MOI) of 1, and intracellular viral RNA was determined (Fig. 4B). The expression of miR-122 significantly increased the amount of the HCV genome in Hec1B, 293T-CLDN, MC-IXC, and RERF-LC-AI cells as well as Huh7 cells and slightly increased it in SK-OV3 and NCI-H-2030 cells. Although the levels of viral RNA in SW620, Caki-2, and SK-PN-DW cells upon expression of miR-122 were higher than those in control cells, no increase of viral RNA was observed. No effect of the expression of miR-122 was observed in 769-P cells. Interestingly, naïve Hec1B cells exhibited a delayed increase in viral RNA from 24 to 48 h postinfection, in contrast to the gradual decrease of viral RNA in other cell lines. Replication of HCV RNA in both naïve and miR-122-expressing Hec1B cells was inhibited by treatment with an inhibitor for HCV protease but not by treatment with IFN-α, due to the lack of an IFN receptor (11), whereas treatments with either IFN-α or the protease inhibitor suppressed the replication of HCV in the other cell lines expressing miR-122 (Fig. 4C). These results indicate that exogenous miR-122 expression enhances the replication of HCV even in nonhepatic cells. Hec1B cells exhibit a delayed replication of HCV, and HCV replication was enhanced by the exogenous expression of miR-122. Therefore, in this study we used Hec1B cells to investigate the biological significance of miR-122 on the replication of HCVcc in nonhepatic cells.

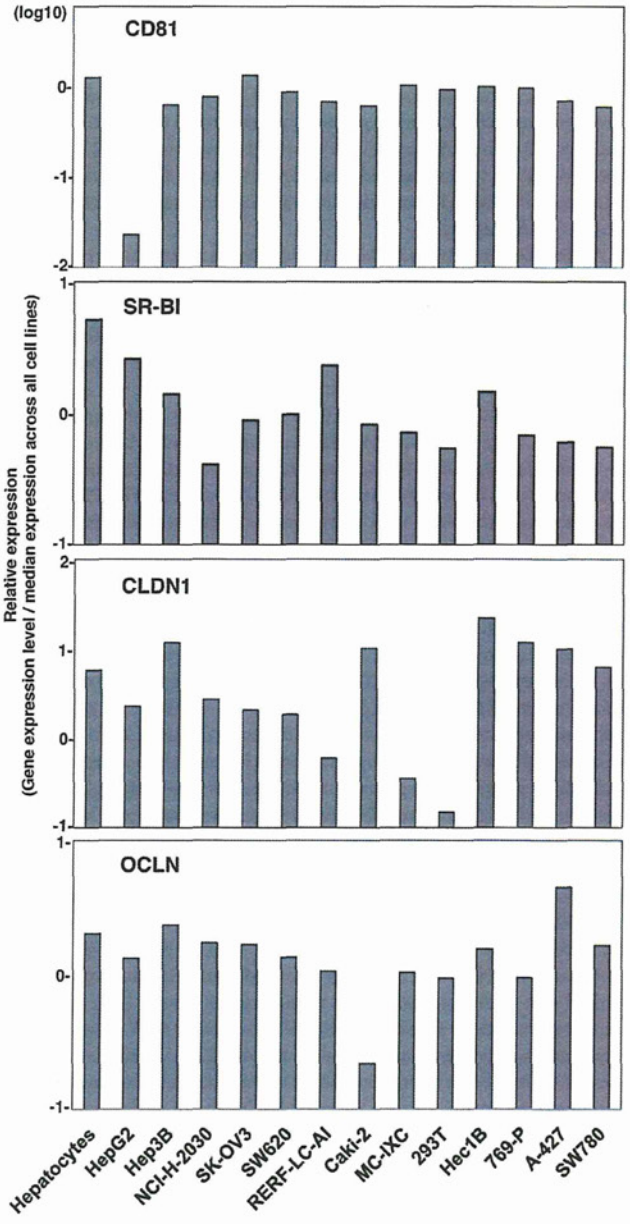

FIG 2 Receptor expression profiling in nonhepatic cells. Relative expression levels of CD81, SR-BI, CLDN1, and OCLN in primary hepatocytes, hepatic cell lines HepG2 and Hep3B, and nonhepatic cells were determined by using the NextBio Body Atlas. Expression levels were standardized by the median expression across all cell lines.

Expression of miR-122 is essential for enhancing HCV replication in Hec1B cells. To confirm the specificity of HCV replication in Hec1B cells, HCVcc was preincubated with an anti-HCV E2 monoclonal antibody, AP-33, or Hec1B/miR-122 and Hec1B/

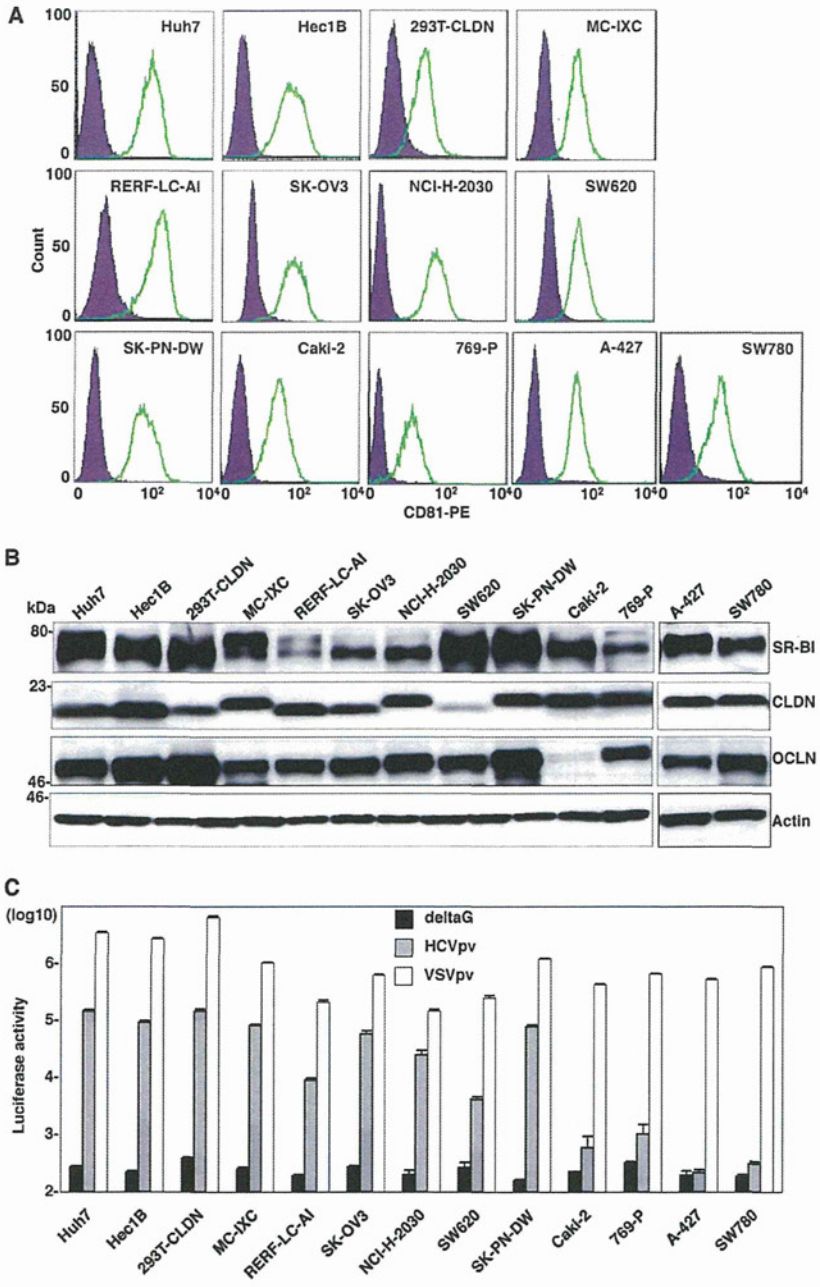

FIG 3 Expression of functional HCV receptor candidates in nonhepatic cells. (A) Expression of hCD81 in nonhepatic cells was determined by flow cytometry. PE, phycoerythrin. (B) Expression levels of SR-B1, CLDN, and OCLN in the nonhepatic cells were determined by immunoblotting. (C) The nonhepatic cell lines were inoculated with pseudotype VSVs bearing no envelope protein (deltaG), HCV envelope proteins of genotype 1b Con1 strain (HCVpv), or VSV G protein (VSVpv), and luciferase expression was determined at 24 h postinfection.

Cont cells were pretreated with anti-hCD81 monoclonal antibody. Replication of HCV RNA was determined upon infection with HCVcc. The antibody treatment significantly inhibited HCV replication in the Hec1B cell line, indicating that HCVcc internalizes into Hec1B cells through a specific interaction between hCD81 and E2 (Fig. 5). Next, we determined the dose dependence of miR-122 expression on the enhancement of HCV replication in Hec1B cells. Huh7.5.1 and Hec1B cells transduced with the lentiviral vector encoding pri-miR-122 were infected with HCVcc at an MOI of 1, and intracellular miR-122 and viral RNA were determined. Expression of miR-122 was increased in Hec1B cells in a dose-dependent manner of the lentivirus, whereas no increase was observed in Huh7.5.1 cells, probably due to the high level of endogenous expression of miR-122 (Fig. 6A, left). HCV RNA replication in Huh7.5.1 and Hec1B cells was correlated with miR-122 expression (Fig. 6A, right), suggesting a close correlation between miR-122 expression and HCV replication.

Next, we examined the expression of viral proteins in Hec1B/

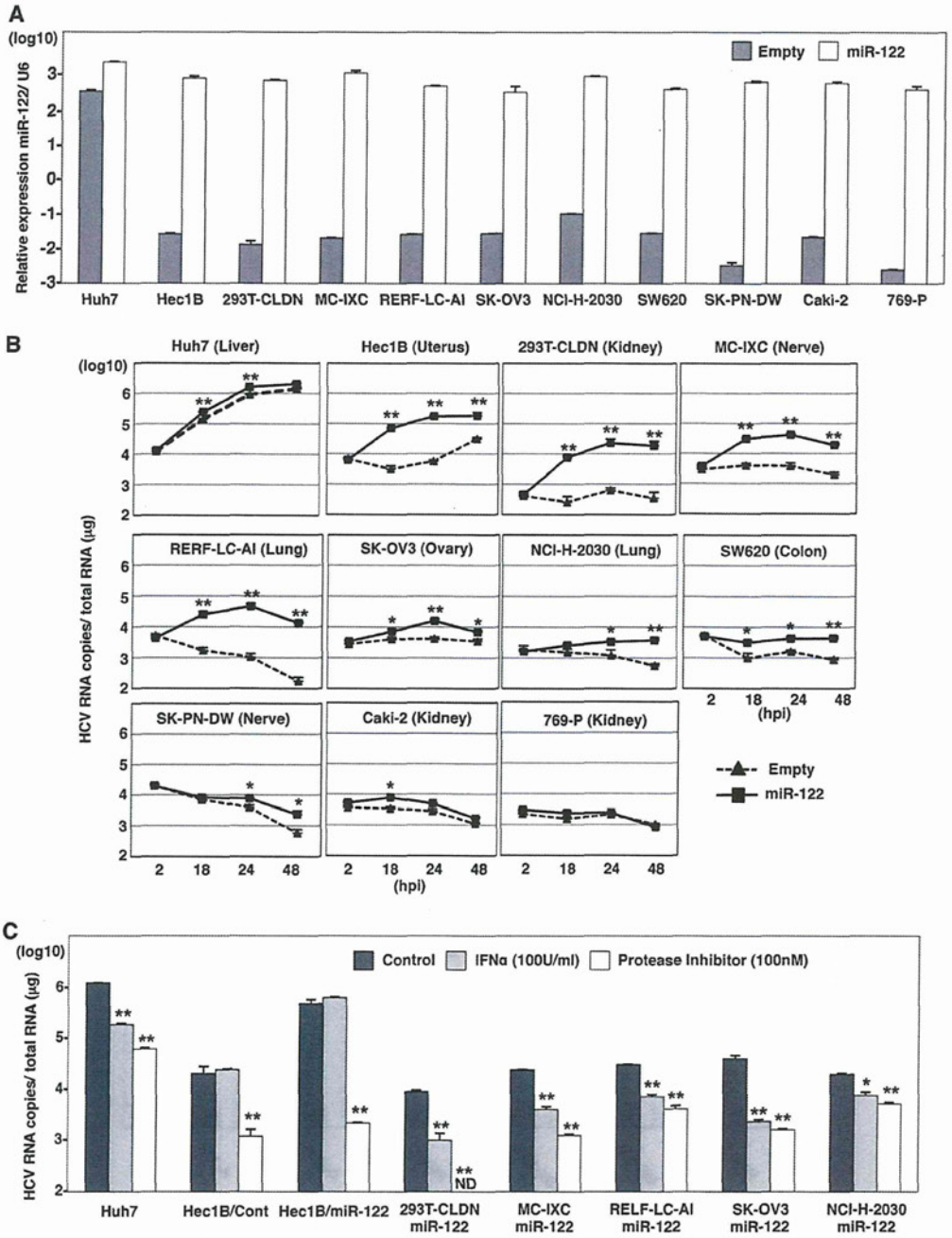

FIG 4 Nonhepatic cell lines susceptible to HCVcc by the expression of miR-122. (A) Exogenous miR-122 was expressed in Huh7, Hec1B, 293T-CLDN, MC-IXC, RERF-LC-AI, SK-OV3, NCI-H-2030, SW620, Caki-2, SK-PN-DW, and 769-P cells by lentiviral vector. Total RNA was extracted from the cells and subjected to qRT-PCR analysis. U6 was used as an internal control. Gray and white bars, endogenous and exogenous levels of miR-122, respectively. (B) HCVcc was inoculated into Huh7 and nonhepatic cell lines expressing (solid lines) or not expressing (dashed lines) exogenous miR-122 at an MOI of 1. Intracellular HCV RNA levels were determined by qRT-PCR at 2, 18, 24, and 48 h postinfection (hpi). (C) Cells were inoculated with HCVcc and simultaneously treated with either 100 U IFN-α or 100 nM HCV protease inhibitor or not treated (control), and intracellular HCV RNA levels were determined by qRT-PCR at 36 h postinfection. Asterisks indicate significant differences (*, $P < 0.05$; **, $P < 0.01$) versus the results for control cells.

miR-122 cells upon infection with HCVcc by immunoblotting and fluorescence microscopic analyses (Fig. 6B). Expression of NS5A protein was increased in Hec1B/miR-122 cells in an MOI-dependent manner. Expression of NS5A in Hec1B/Cont cells infected with HCVcc at an MOI of 3 was significantly lower than that in Hec1B/miR-122 cells infected with HCVcc at an MOI of 0.5. HCV core and NS proteins were shown to localize mainly on the lipid droplets and cytoplasmic face of the endoplasmic reticulum (ER) in Huh7 and Hep3B/miR-122 cells infected with HCVcc (29, 40). Immunofluorescence analyses revealed that HCV core and NS5A proteins were colocalized with lipid droplets and calnexin, an ER marker, in Hec1B cells infected with HCVcc (Fig. 7).

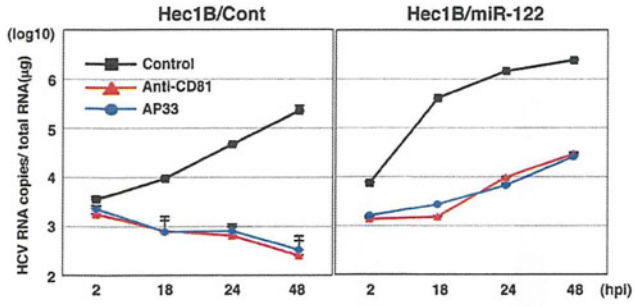

FIG 5 Neutralization of HCVcc infection in Hec1B cells by specific antibodies. HCVcc was preincubated with anti-E2 antibody (AP-33) and inoculated into Hec1B/Cont and Hec1B-miR-122 cells. Cells were preincubated with anti-human CD81 antibody and inoculated with HCVcc. Intracellular HCV RNA levels at 2, 18, 24, and 48 h postinfection were determined by qRT-PCR.

To further confirm the specificity of the enhancement of HCV replication by the expression of miR-122, Huh7, Hec1B/miR-122, and Hec1B/Cont cells were treated with LNAs that were either specific to miR-122 (LNA-miR-122) or nonspecific (LNA-control) at 6 h before infection with HCVcc. Although the treatment with LNA-miR-122 inhibited the enhancement of viral RNA replication in Huh7 and Hec1B/miR-122 cells in a dose-dependent manner, no inhibition of viral replication was observed in Hec1B/Cont cells (Fig. 6C). These results suggest that Hec1B cells permit HCV replication in a miR-122-independent manner and exogenous expression of miR-122 enhances viral replication.

Specific interaction between miR-122 and the 5′ UTR of HCV is required for HCV replication. To determine the effect of the specific interaction between miR-122 and the 5′ UTR of the HCV genome on the enhancement of RNA replication, we generated MT pri-miR-122 carrying a substitution of uridine to adenosine in the seed domain and an additional complementary substitution of adenosine to uridine to stabilize the loop structure of pri-miR-122 (Fig. 8A). A high expression level of MT miR-122, comparable to that of WT miR-122, was introduced into Hec1B cells by infection with lentiviral vectors (Fig. 8B). To determine the specificity of miR-122 on the replication of HCV, Hec1B cells expressing either WT or MT miR-122 were inoculated with HCVcc at an MOI of 1. Enhancement of HCV replication was observed in Hec1B cells by the expression of WT but not that of MT miR-122, suggesting that the sequence specificity of miR-122 with the 5′ UTR of HCV is crucial for the efficient replication of HCV (Fig. 8C). To further confirm the effect of the specificity of interaction between miR-122 and the binding sites in the 5′ UTR of HCV on the enhancement of HCV replication, we generated two mutant viruses, HCVcc-M1 and HCVcc-M2, carrying complementary substitutions in the miR-122-binding site 1 alone and in both sites 1 and 2 in the 5′ UTR of HCV, respectively (Fig. 8D). Recently, Jangra et al. demonstrated that the propagation of a mutant HCVcc bearing mutations in sites 1 and 2 in the 5′ UTR was rescued by the expression of MT miR-122 in Huh7.5 cells (25). We confirmed that the propagation of HCVcc-M1 and HCVcc-M2 in Huh7.5.1 cells was rescued by the expression of MT miR-122 but not of WT miR-122, although the recovery of infectious titers of HCVcc-M2 was significantly lower than the recovery of infectious titers of HCVcc-M1 (Fig. 8E). Next, to examine the interaction between miR-122 and the HCV genome in Hec1B cells, we inoculated HCVcc or mutant viruses into Hec1B cells expressing either or both WT and MT miR-122 and determined the replication of HCV RNA by qRT-PCR (Fig. 8F). Expression of WT and MT miR-122 in Hec1B cells permits replication of HCVcc and HCVcc-M2, respectively, although the enhancing effects differed. On the other hand, the expression of both WT and MT miR-122 is required for the replication of HCVcc-M1, because MT and WT miR-122 bind to sites 1 and 2 in the 5′ UTR of this virus, respectively. Interestingly, a low level of HCVcc-M1 replication was also observed in Hec1B cells expressing either WT or MT miR-122, in contrast to the requirement of the corresponding miR-122 for the replication of HCVcc and HCVcc-M2. These results suggest that the specific interaction between miR-122 and the 5′ UTR of HCV is crucial for the replication of HCV.

Viral particle formation in hepatic and nonhepatic cells. These data suggest that miR-122 expression facilitates replication of HCV RNA in nonhepatic cells. Recently, we have shown that expression of miR-122 facilitates infectious particle formation of HCVcc in a hepatoma cell line, Hep3B (29). To examine the effect of miR-122 expression on particle formation in nonhepatic cells, intracellular and extracellular viral RNA levels in cells infected with HCVcc were determined. Intracellular RNA replication in the hepatic cell lines, including Huh7.5.1 and Hep3B/miR-122, was increased up to 72 h postinfection with HCVcc, whereas in nonhepatic cell lines, including 293T-CLDN/miR-122 and Hec1B/miR-122, such replication was comparable to that in the hepatic cell lines until 24 h postinfection but reached a limit at this point (Fig. 9A). In spite of no clear increase of intracellular HCV RNA in Hep3B/Cont cells upon infection with HCVcc (Fig. 9A), subtle but substantial production of infectious particles was detected in the culture supernatants at 72 h postinfection, in contrast to no production of infectious particles in those of the nonhepatic cell lines (Fig. 9B). Furthermore, no focus formation was observed in Hec1B/miR-122 cells upon infection with HCVcc, in contrast to the many foci in Huh7.5.1 cells (Fig. 9C), and no infectivity was detected even in the lysates of Hec1B/miR-122 cells infected with HCVcc (Fig. 9D). These results suggest that not only the replication efficiency of viral RNA but also other factors are involved in the assembly of HCV and that the viral assembly process is impaired in Hec1B/miR-122 cells infected with HCVcc, in spite of the efficient replication of HCV RNA.

It was previously shown that lipid droplets, diacylglycerol *O*-acyltransferase 1 (DGAT1), and apolipoproteins B and E play an important role in the assembly of HCV particles (10, 22, 40). To understand the molecular mechanisms underlying the low efficiency of infectious particle formation in nonhepatic cells, we first examined the subcellular localization of lipid droplets and HCV core protein in Hec1B/miR-122 cells infected with HCVcc. Although the core protein was detected around the lipid droplets, as seen in Huh7.5.1 cells, only a small amount of lipid droplets was detected in Hec1B/miR-122 cells infected with HCVcc compared with the amount detected in Huh7.5.1 cells (Fig. 9E), suggesting that the low level of lipid droplet formation is involved in the impairment of infectious particle formation in nonhepatic cells.

Next we examined the expression patterns of molecules involved in lipid metabolism by using cDNA microarray and qPCR analyses. Although expression levels of low-density lipoprotein receptor (LDLR), sterol regulatory element-binding protein 1c (SREBP1c), SREBP2, and DGAT1 in nonhepatic Hec1B and 293T cells were comparable to those in hepatic Huh7 and Hep3B cells, those of VLDL-associated proteins, including ApoE, ApoB, and

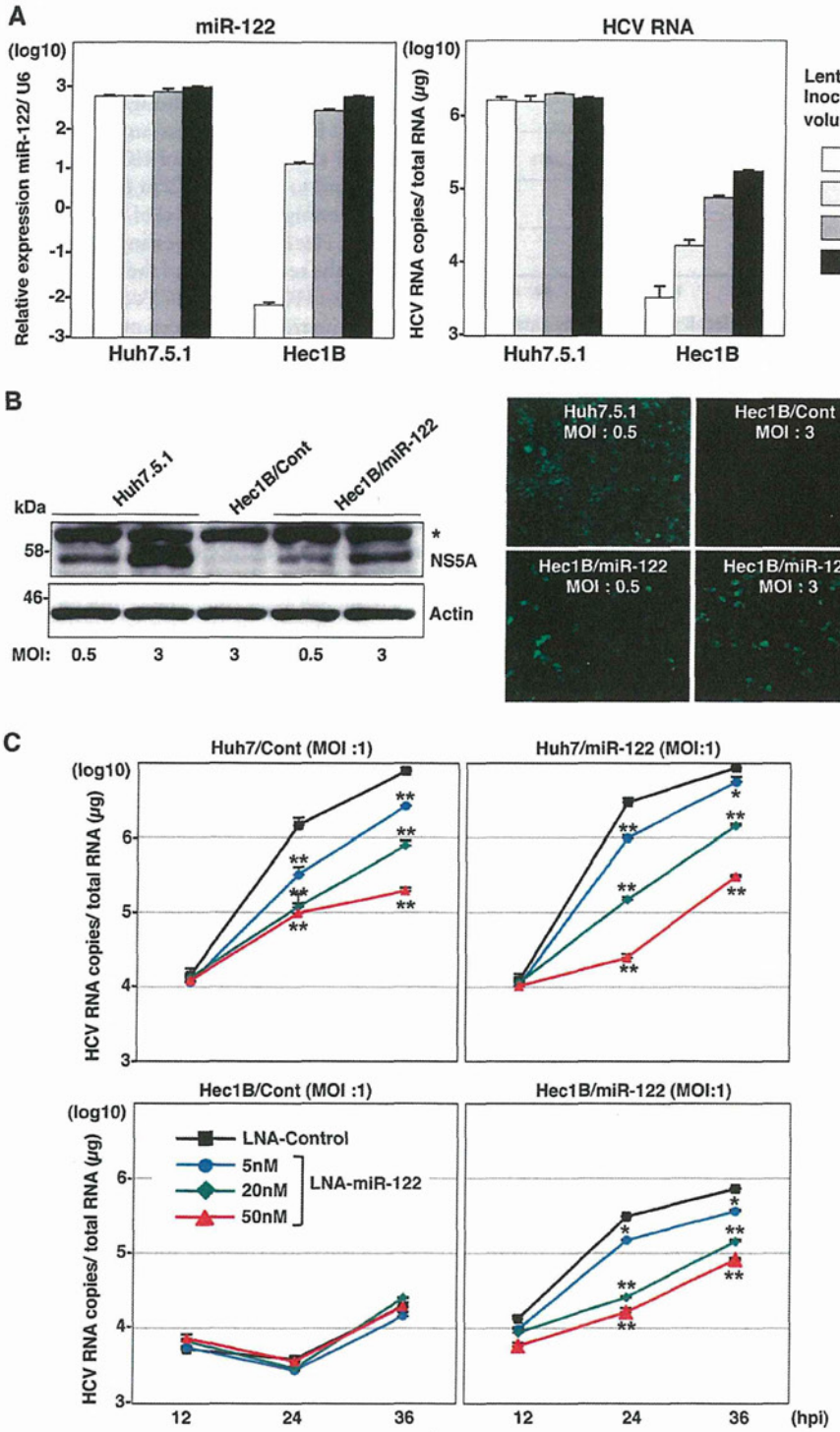

FIG 6 Expression of miR-122 is essential for the enhancement of HCV replication in the Hec1B cells. (A) Huh7.5.1 and Hec1B cells were transduced with lentiviral vectors expressing miR-122 in a dose-dependent manner and infected with HCVcc at an MOI of 1. Intracellular miR-122 and HCV RNA were determined at 24 h postinfection by qRT-PCR. (B) Huh7.5.1 and Hec1B/miR-122 cells were infected with HCVcc at an MOI of 0.5 or 3 and subjected to immunoblotting and immunofluorescence analyses using anti-NS5A antibodies at 48 h postinfection. The asterisk indicates nonspecific bands. (C) LNAs specific to miR-122 at a final concentration of 5 nM, 20 nM, or 50 nM and control (LNA alone at 50 nM) were introduced into Huh7/Cont, Huh7/miR-122, Hec1B/miR-122, and Hec1B/Cont cells by using Lipofectamine RNAiMAX transfection reagent and infected with HCVcc at an MOI of 1 at 6 h posttransfection. Intracellular HCV RNA levels were determined by qRT-PCR at 12, 24, and 36 h postinfection. Asterisks indicate significant differences (*, $P < 0.05$; **, $P < 0.01$) versus the results for control cells.

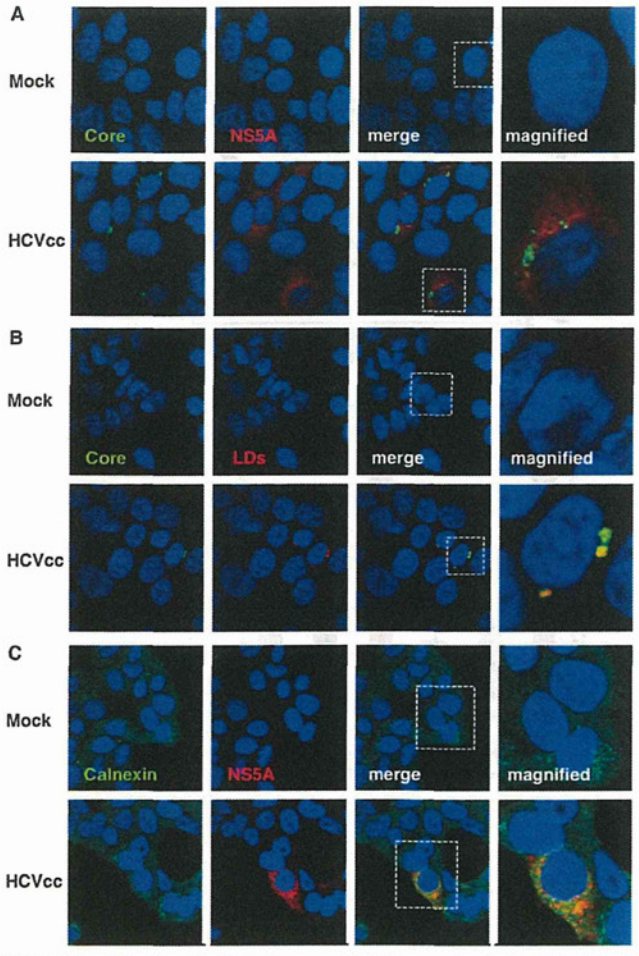

FIG 7 Subcellular localization of core and NS5A proteins in Hec1B/miR-122 cells infected with HCVcc. Hec1B/miR-122 cells infected with or without HCVcc at an MOI of 1 were fixed with 4% PFA at 48 h postinfection and stained with appropriate antibodies to core and NS5A proteins (A), core protein and lipid droplets (B), and NS5A and calnexin (C). The boxes in the merged images were magnified, and the images are displayed on the right.

MTTP, in nonhepatic cells were significantly lower than those in hepatic cells (Fig. 10). Collectively, these results suggest that intracellular functional lipid metabolism, including the biosynthesis of lipid droplets and the production of VLDL, participates in the assembly of HCV.

Establishment of HCV replicon in Hec1B/miR-122 cells. It was previously shown by using RNA replicon cells based on the JFH1 strain that expression of miR-122 enhanced the translation of HCV RNA in HEK293 cells and MEFs (8, 35). We tried to establish HCV replicon cells based on genotype 1b Con1 and genotype 2a JFH1 strains in Hec1B/miR-122 and HEK293 cells stably expressing miR-122 (HEK293/miR-122). To examine the colony formation efficiency of the HCV RNAs of the Con1 and JFH1 strains, SGR RNA was electroporated into the cell lines and selected by G418 for 3 weeks. Expression of miR-122 in Hec1B cells significantly enhanced the colony formation of SGR of the Con1 strain (Fig. 11A), suggesting that the expression of miR-122 in Hec1B cells supports the efficient replication of SGR. HCV replication in 20 replicon clones established by the transfection with SGR RNA of the Con1 strain in Hec1B/miR-122 cells was examined by qRT-PCR and immunoblotting. All clones contained high levels of HCV RNA (3×10^6 to 5×10^7 copies per μg of total RNA) (Fig. 11B), and expression of NS5A was well correlated with the levels of HCV RNA in the clones (Fig. 11C). Two replicon clones (clones 2 and 10) in Hec1B/miR-122 cells exhibiting high levels of RNA replication and NS5A expression further confirmed the high level of expression of NS5A by immunofluorescent microscopy (Fig. 11D). These results suggest that expression of miR-122 facilitates the efficient replication of SGR of at least two HCV genotypes in Hec1B cells.

Our previous reports showed that HCV NS proteins were colocalized with dsRNA and cochaperone molecules, FK506-binding protein 8 (FKBP8), in dot-like structures on the ER membrane of Huh7 replicon cells (59). Colocalization of NS5A with dsRNA or FKBP8 was observed in the dot-like structures in not only Huh7 SGR cells but also Hec1B/miR-122 SGR cells (Fig. 12A), suggesting that the dot-like structure required for efficient viral replication is also generated in Hec1B/miR-122 replicon cells. It has been shown that HCV replication induces the formation of convoluted membranous structures, called membranous webs, in Huh7 cells (13, 45). FM-EM techniques revealed the localization of NS5A on the convoluted structures in Hec1B/miR-122 replicon cells (Fig. 12B). These results suggest that the replication complex required for viral replication was also generated in the Hec1B/miR-122 replicon cells, as was seen in the Huh7 replicon cells.

miR-122 is a crucial determinant of HCVcc propagation. It has been shown that the infectivity of HCVcc in cured cells, established when IFN treatment induces the elimination of the viral genome from the Huh7 replicon cells harboring an HCV RNA, is significantly higher than that in parental Huh7 cells (2, 66). Therefore, we tried to establish Hec1B-based cured cells from the Con1 SGR clones harboring a high copy number of HCV RNA. Treatment with cyclosporine and the protease inhibitor of HCV suppressed NS5A expression in Hec1B/miR-122 SGR clone 2 in a dose-dependent manner (Fig. 13A), whereas no reduction was observed by the IFN treatment due to a lack of an IFN receptor, as shown in Fig. 4C. It was reported that monotherapy by the HCV protease inhibitor induces the emergence of resistant breakthrough viruses (34, 55). Therefore, we treated five Hec1B/miR-122 SGR clones (clones 2, 5, 10, 14, and 16) with 1 μg/ml cyclosporine and 100 nM protease inhibitor for HCV. Viral RNA was determined by qRT-PCR every 5 days posttreatment. Elimination of viral RNA was achieved in four clones (clones 2, 5, 10, and 14) within 20 days posttreatment (Fig. 13B). Replication of HCV RNA in the cured cells infected with HCVcc at an MOI of 0.5 was 2- to 30-fold higher than that in parental cells at 24 h postinfection (Fig. 13C). In addition, replication of HCV RNA in cured clone 2 infected with HCVcc at an MOI of 0.1 was comparable to that in Huh7.5.1 cells until 24 h postinfection (Fig. 13D). Expression of NS5A was significantly increased in cured clone 2 compared to that in the parental Hec1B/miR-122 cells (Fig. 13E and F). It was previously shown that the increased permissiveness of Huh7-derived cured cells, Huh7.5 cells, is attributable to a mutation in the RIG-I gene (58). To examine the innate immune response in the parental and cured Hec1B/miR-122 cells, induction of IFN-stimulated gene 15 (ISG15) was determined upon stimulation with IFN-α or VSV. Although induction of ISG15 was not observed in either parental or cured cells upon stimulation with IFN-α due to a lack of an IFN receptor (11) (Fig. 14A), it was

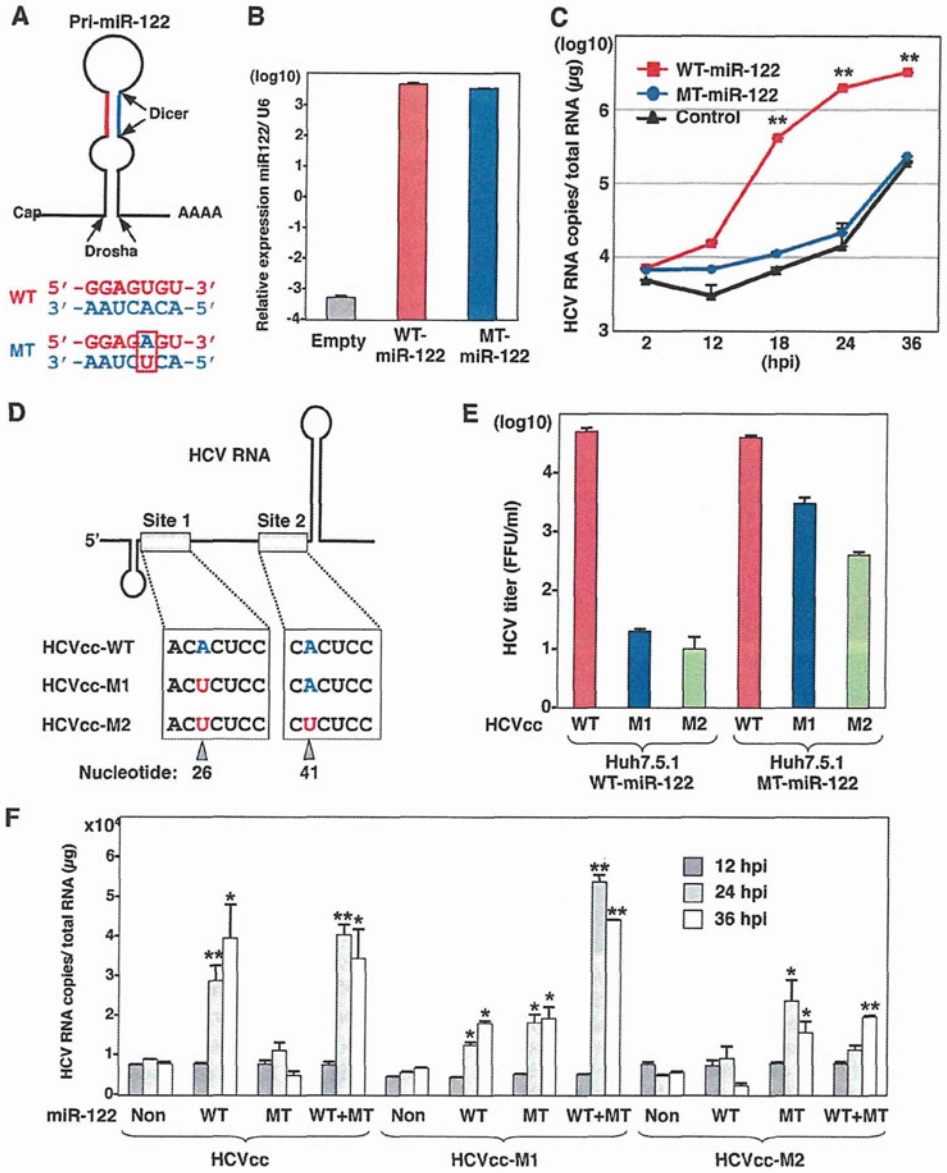

FIG 8 Specific interaction between miR-122 and the 5′ UTR of HCV is required for HCV replication. (A) Structures of pri-miR-122 and the nucleotide sequences of WT and MT miR-122, which has a substitution of uridine to adenosine in the seed domain and an additional complementary substitution of adenosine to uridine for stable expression. (B) WT or MT miR-122 was introduced into Hec1B cells by a lentiviral vector, and miR-122 expression levels were determined by qRT-PCR. (C) HCVcc was inoculated into Hec1B cells expressing either WT or MT miR-122 and control cells at an MOI of 1, and the intracellular HCV RNA levels were determined by qRT-PCR. (D) Diagram of mutant viruses HCVcc-M1 and HCVcc-M2 carrying complementary substitutions in the miR-122-binding site 1 alone and both sites 1 and 2 in the 5′ UTR of HCV, respectively. (E) Viral RNA of HCVcc, HCVcc-M1, or HCVcc-M2 was electroporated into Huh7.5.1 cells expressing either WT or MT miR-122, and infectious titers of the viruses recovered in the culture supernatants at 72 h postinfection of the second passage were determined by a focus-forming assay in cells expressing either WT or MT miR-122. Red, blue, and green bars, infectious titers of HCVcc, HCVcc-M1, and HCV-M2, respectively. (F) HCVcc, HCVcc-M1, or HCV-M2 was inoculated into Hec1B cells expressing either or both WT and MT miR-122 at an MOI of 0.5, and intracellular HCV RNA levels were determined at 12, 24, and 36 h postinfection by qRT-PCR. Asterisks indicate significant differences (*, $P < 0.05$; **, $P < 0.01$) versus the results for control cells.

detected in both cells infected with VSV (Fig. 14B). Therefore, other mechanisms should be involved in the enhancement of permissiveness of Hec1B-derived cured cells. Ehrhardt et al. showed that the expression levels of miR-122 in Huh7-derived cured cells, including Huh7.5, Huh7.5.1, and Huh7-Lunet cells, are significantly higher than those in parental Huh7 cells (14). In addition, our recent study indicated that levels of expression of miR-122 in the cured Huh7 and Hep3B/miR-122 cells were higher than those in parental cells (29). Levels of expression of miR-122 in the Hec1B-based cured cell clones are also higher than those in parental Hec1B/miR-122 cells (Fig. 13G). These results suggest that a high level of miR-122 expression is a crucial determinant of high susceptibility to HCVcc propagation in the cured cells.

JVI
Journals.ASM.org

CD44 Participates in IP-10 Induction in Cells in Which Hepatitis C Virus RNA Is Replicating, through an Interaction with Toll-Like Receptor 2 and Hyaluronan

Takayuki Abe,[a]* Takasuke Fukuhara,[a] Xiauyu Wen,[a]* Akinori Ninomiya,[a] Kohji Moriishi,[c] Yoshihiko Maehara,[d] Osamu Takeuchi,[b] Taro Kawai,[b] Shizuo Akira,[b] and Yoshiharu Matsuura[a]

Department of Molecular Virology, Research Institute for Microbial Diseases,[a] and Laboratory of Host Defense, WPI Immunology Frontier Research Center,[b] Osaka University, Osaka, Department of Microbiology, Faculty of Medicine, Yamanashi University, Yamanashi,[c] and Department of Surgery and Science, Graduate School of Medical Sciences, Kyushu University, Fukuoka, Japan[d]

The mechanisms of induction of liver injury during chronic infection with hepatitis C virus (HCV) are not well understood. Gamma interferon (IFN-γ)-inducible protein 10 (IP-10), a member of the CXC chemokine family, is expressed in the liver of chronic hepatitis C (CHC) patients and selectively recruits activated T cells to the sites of inflammation. Recently, it was shown that a low plasma concentration of IP-10 in CHC patients was closely associated with the outcome of antiviral therapy. In this study, we examined the role of the Toll-like receptor (TLR) pathway on IP-10 production in cells replicating HCV. Among the CXC chemokines, the expression of IP-10 was specifically increased in cells replicating HCV upon stimulation with conventional TLR2 ligands. The enhancement of IP-10 production upon stimulation with TLR2 ligands in cells replicating HCV induced CD44 expression. CD44 is a broadly distributed type I transmembrane glycoprotein and a receptor for the glycosaminoglycan hyaluronan (HA). In CHC patients, the expression of HA in serum has been shown to increase in accord with the progression of liver fibrosis, and HA also works as a ligand for TLR2. In the present study, IP-10 production upon HA stimulation was dependent on the expression of TLR2 and CD44, and a direct association between TLR2 and CD44 was observed. These results suggest that endogenous expression of HA in hepatocytes in CHC patients participates in IP-10 production through an engagement of TLR2 and CD44.

Hepatitis C virus (HCV) infects 170 million people worldwide and frequently leads to the development of cirrhosis and hepatocellular carcinoma (32). The current combination therapy of pegylated interferon (IFN) and ribavirin is effective in fewer than 50% of patients infected with HCV of genotype 1. Histological analyses of the liver biopsy specimens of chronic hepatitis C (CHC) patients have revealed the infiltration of mononuclear cells, including T and B lymphocytes, natural killer (NK) and NKT cells, and virus-specific cytotoxic T lymphocytes (2, 26, 42, 47). Long-term infection by HCV is associated with progressive infiltration of the liver parenchyma by the mononuclear cells, fibrosis, cirrhosis, and, finally, the development of hepatocellular carcinoma. Although the factors that regulate the recruitment of mononuclear cells and the other components of the inflammatory response to the HCV-infected liver cells are not well characterized, it has been hypothesized that chemokines and other inflammatory cytokines play fundamental roles in the immune cell recruitment.

Chemokines, small chemotactic cytokines (approximately 8 to 10 kDa) that act to guide leukocytes to sites of inflammation, are important determinants of the development of intrahepatic inflammation in chronic HCV infection (16). Although chemokines play crucial roles in viral elimination, persistent expression of chemokines may induce tissue damage and inflammation in chronic infection. CXCR3 is a receptor for the CXC chemokines, including IP-10 (also known as CXCL10), MIG (also known as CXCL9), and I-TAC (also known as CXCL11). Recent studies have shown that the CXCR3 ligands are elevated in the livers and sera of CHC patients (12–14, 17, 33, 36, 40, 49), and IP-10 was shown to correlate with treatment response. In addition, several studies suggested a significant association between the expression of the CXC chemokines and the development of progressive liver injury in CHC patients (23, 49). In CHC patients, these chemokines are expressed in hepatocytes, hepatic stellate cells, and sinusoidal endothelial cells (12, 14, 33, 42, 49), and the majority of intrahepatic mononuclear cells express CXCR3, suggesting that the CXC chemokine network plays a pivotal role in the migration of mononuclear cells to the liver and in the subsequent intrahepatic inflammation.

Among chemokines, IP-10 plays a central role in liver inflammation, and it is expressed in the liver of hepatitis C patients (12, 33, 42). Several independent studies indicate that elevated plasma levels of IP-10 predict the failure of combination therapy (3, 5, 40). In addition, a recent study suggests that IP-10 in the plasma of many hepatitis C patients is cleaved by DPP4 (also known as CD26) and that the truncated IP-10 works as an IP-10 receptor antagonist (4). In contrast to these clinical observations, little is known about the expression of the CXC chemokines in cells replicating HCV.

Production of the inflammatory chemokines upon viral infec-

Received 21 November 2011 Accepted 23 March 2012
Published ahead of print 4 April 2012
Address correspondence to Yoshiharu Matsuura, matsuura@biken.osaka-u.ac.jp.
* Present address: Takayuki Abe, Department of Medicine, University of Miami School of Medicine, Miami, Florida, USA; Xiauyu Wen, Department of Hepatology, The First Hospital of Jilin University, Changchun, Jilin Province, China.

doi:10.1128/JVI.06872-11